

Evolutionary Multi-Objective Day-Ahead Thermal Generation Scheduling in Uncertain Environment

Anupam Trivedi, *Student Member, IEEE*, Dipti Srinivasan, *Senior Member, IEEE*, Deepak Sharma, *Member, IEEE*, and Chanan Singh, *Fellow, IEEE*

Abstract—This paper addresses day-ahead thermal generation scheduling as a realistic multi-objective optimization problem in an uncertain environment considering system operation cost, emission cost and reliability as the multiple objectives. The uncertainties occurring due to unit outage and load forecast error are incorporated using loss of load probability (LOLP) and expected unserved energy (EUE) reliability indices. For solving the above-mentioned scheduling problem, a multi-objective generation scheduling algorithm (MOGSA) is proposed in this paper. Three case studies are performed on large scale test systems considering two different bi-objective optimization models and a three-objective optimization model that may be chosen by the system operator according to his/her own preference. The simulation results demonstrate the advantages of solving the thermal generation scheduling problem as a realistic multi-objective optimization problem in an uncertain environment. Finally the authors suggest a systematic procedure for the system operators to choose a single solution for the thermal generation scheduling problem.

Index Terms—Evolutionary multi-objective optimization, thermal generation scheduling, unit commitment, uncertainty.

NOMENCLATURE

T_{max}	Number of hours in dispatch period.
T	Hourly time index.
N	Number of generating units.
i	Generating unit index.
P_i^t	Power generated by unit i at hour t .
$P_{max,i}$	Rated upper limit generation of unit i .
$P_{min,i}$	Rated lower limit generation of unit i .
f_i^t	Fuel cost of i th unit at hour t in \$/h.
SU_i^t/SD_i^t	Start-up/shut-down cost of unit i at hour t .

L^t	Load demand at hour t .
MUT/MDT	Minimum up/down time of unit i .
a_i, b_i, c_i	Fuel cost coefficients of the i th generator.
a_{1i}, b_{1i}, c_{1i}	Emission cost coefficients of the i th generator.

I. INTRODUCTION

THE day-ahead thermal generation scheduling (TGS) problem plays a major role in the daily operational planning of power systems. It involves two scheduling tasks: 1) unit commitment (UC) which determines the on/off schedules of the generators and 2) electrical power dispatch (or load dispatch) which optimally distributes the forecasted load among the committed generators. The TGS requires effectively performing the above two tasks to meet the forecasted load demand over a particular time horizon, satisfying a large set of operating constraints and achieving certain objectives [1]. Most of the approaches in the literature solve TGS considering cost as the single (economic) objective and the problem is known as the classical UC problem. However, due to increasing environmental concerns that arise from the emissions produced by fossil-fuel based thermal power plants, the economic objective can no longer be considered alone. Moreover, TGS involves uncertainty in generator availability and load forecast data. However, the UC problem is usually solved in deterministic environment. System operator (SO) would nevertheless prefer to obtain more reliable generation schedule by incorporating various uncertainties.

Over the last two decades, considerable research has been conducted using AI techniques to solve the UC problem. The techniques include genetic algorithm (GA) [2], [3], memetic algorithm (MA) [4], particle swarm optimization (PSO) [5] and simulated annealing (SA) [6]. Evolutionary algorithms like evolutionary programming (EP) [7] and PSO [8] have found application in the solution of economic load dispatch (ELD) problem too. In the last few years, the scheduling of electrical power dispatch for emission and economic objectives has drawn much attention. This is known as the multi-objective environmental/economic dispatch (EED) problem. Non-dominated sorting genetic algorithm (NSGA) [9], fuzzified MOPSO [10] and MOPSO with fuzzy clustering [11] have been successfully implemented to solve the multi-objective EED problem.

The above mentioned studies and most of the other UC, ELD and EED studies in the literature use deterministic models,

Manuscript received February 25, 2012; revised August 14, 2012; accepted September 22, 2012. Date of publication November 15, 2012; date of current version April 18, 2013. This work was supported by Singapore National Research Foundation, Grant No.: R-263-000-522-272. Paper no. TPWRS-00109-2012.

A. Trivedi and D. Srinivasan are with the Department of Electrical and Computer Engineering, National University of Singapore, Singapore 117576 (e-mail: serat@nus.edu.sg; elesd@nus.edu.sg).

D. Sharma is with the Department of Mechanical Engineering, Indian Institute of Technology Guwahati, India 781039 (e-mail: dsharma@iitg.ernet.in).

C. Singh is with the Department of Electrical and Computer Engineering, Texas A&M University, College Station, TX 77843 USA (e-mail: singh@ece.tamu.edu).

Color versions of one or more of the figures in this paper are available online at <http://ieeexplore.ieee.org>.

Digital Object Identifier 10.1109/TPWRS.2012.2222939

which are not able to reflect some real situations like uncertainties in load demand, fuel prices and unit availability. Reference [12] presented an improved PSO method with stochastic model to deal with the EED problem. The stochastic model considered the uncertainty related to fuel cost coefficients, emission coefficients and load demand. In [13], the UC problem was addressed considering generator outages through a mixed-integer PSO algorithm. To account for the generator outages, a reliability requirement was incorporated into the spinning reserve constraint. The study [14] included the uncertainties due to unit outage and load forecast error in the UC problem by implementing reliability constraints on LOLP and EUE reliability indices and the reliability constrained UC problem was solved using an SA based algorithm.

The literature suggests that many studies exist for the UC, ELD and EED problems. However, to the best of the authors' knowledge there are no studies that have addressed the day-ahead TGS problem in uncertain environment for important objectives like reliability and emission along with the economic objective.

In this paper, the TGS problem is addressed as a realistic multi-objective optimization (MOO) problem in uncertain environment. The uncertainties due to unit outage and load forecast error are incorporated with the help of LOLP and EUE reliability indices [14]. Three multi-objective case studies are performed on the TGS problem in uncertain environment by considering different optimization models and extending our earlier proposed algorithm [1].

The main contribution of this paper is in demonstrating the advantages of solving the day-ahead TGS as a realistic MOO problem in uncertain environment. Moreover, this paper presents three different MOO models that may be chosen by the SO according to his/her own preference. Additionally, in the end, the authors' suggest the best optimization model and a systematic method for the SO to choose a single solution from the trade-off Pareto-optimal solutions that are obtained for the multi-objective TGS problem.

The multi-objective TGS problem is formulated in Section II. Thereafter, the proposed algorithm is described in Section III. The results and discussions are presented in Section IV followed by quantitative performance assessment of the proposed algorithm in Section V and the paper is concluded in Section VI.

II. MULTI-OBJECTIVE THERMAL GENERATION SCHEDULING: PROBLEM FORMULATION

In this section, the multiple objectives in the TGS problem and the associated constraints are presented.

A. Objective Functions

1) *System Operation Cost*: The total system operating cost includes the fuel cost of the committed generators and the transition cost over the entire scheduling horizon:

$$F_1 = \sum_{t=1}^{T_{max}} \sum_{i=1}^N (f_i^t + SU_i^t + SD_i^t). \quad (1)$$

The fuel cost f_i^t of unit i is expressed as the quadratic function of its power output during hour t :

$$f_i^t = a_i(P_i^t)^2 + b_i(P_i^t) + c_i. \quad (2)$$

The transition cost is the sum of start-up costs and shut-down costs.

2) *Reliability*: In this paper, the expected unserved energy (EUE) index which expresses the expected amount of energy not supplied by the generation system during the scheduling horizon is used as a measure of reliability of the system. The objective function F_2 is equal to the EUE index itself. The procedure for calculating the EUE index is presented later in the paper.

3) *Emission Cost*: The objective function representing the emission cost is similar to the function representing the fuel cost of generators:

$$F_3 = \sum_{t=1}^{T_{max}} \sum_{i=1}^N (a_{1i}(P_i^t)^2 + b_{1i}(P_i^t) + c_{1i}). \quad (3)$$

B. Constraints

The solution must satisfy several constraints as follows:

1) *System power balance*: the total power generation at hour t must be equal to the load demand for that hour:

$$\sum_{i=1}^N P_i^t = L^t, \quad t = 1, 2, \dots, T_{max}. \quad (4)$$

2) *Unit minimum up/down time*: if a unit is on/off, it must remain on/off for at least MUT/MDT time duration.

3) *Unit generation limits*: for stable operation, the power output of each generator is restricted within limits as follows:

$$P_{min,i} \leq P_i^t \leq P_{max,i}. \quad (5)$$

4) The LOLP reliability constraint is incorporated as

$$LOLP_t \leq L_{max}, \quad t \in [1, T] \quad (6)$$

where $LOLP_t$ is the LOLP for hour t and L_{max} is the user-defined maximum allowed limit of the LOLP reliability index. It is noted that the LOLP is the probability that the generation system will not cover the forecasted demand.

5) The EUE reliability constraint is incorporated as

$$EUE_{tot} \leq E_{max} \quad (7)$$

where EUE_{tot} is the total expected unserved energy for the entire scheduling period and E_{max} is the user-defined maximum allowed limit of the EUE reliability index. It is noted that EUE is incorporated as a reliability constraint only in case study 2 when the objectives are system operation cost and emission cost. In case study 1 and 3, EUE index is considered as an objective and not as a constraint.

6) The constraint related to maximum system operation cost is incorporated as

$$F_1 \leq Cost_{max} \quad (8)$$

where $Cost_{max}$ is the user-defined upper limit for solution's system operation cost. It is noted that this constraint is incorporated only in case study 3.

7) The constraint related to maximum emission cost is incorporated as

$$F_3 \leq Emission_{max} \quad (9)$$

where $Emission_{max}$ is the user-defined upper limit for solution's emission cost. It is noted that this constraint [like constraint (8)] is incorporated only in case study 3.

III. PROPOSED ALGORITHM FOR THERMAL GENERATION SCHEDULING IN UNCERTAIN ENVIRONMENT

In this paper, our earlier proposed algorithm [1] has been extended to solve the multi-objective TGS problem in uncertain environment. It is noted that the proposed algorithm is referred as multi-objective generation scheduling algorithm (MOGSA) in this paper. The uncertainties due to unit outage and load-forecast error have been incorporated in the solution with the help of reliability indices LOLP and EUE. The details of MOGSA and the calculation of LOLP and EUE indices are presented in the following sections.

A. Chromosome Formulation

For every chromosome, an $N \times T_{max}$ binary unit commitment matrix (UCM) is used to represent the generator on/off status and an $N \times T_{max}$ real power matrix (RPM) is used to represent the corresponding power dispatch. It is noted that a chromosome's actual generation schedule is represented by its resultant power matrix (Res.PM) which is obtained by multiplying the corresponding elements of UCM and RPM.

B. Generation of Initial Population

All chromosomes in the initial population are generated randomly. UCM of each chromosome is a randomly generated binary matrix. In RPM of each chromosome, the power dispatch of each generator is generated randomly within the power limits of that generator.

C. Calculation of Reliability Indices

In this subsection, the procedure for calculation of reliability indices is explained for cases when only uncertainty due to unit outage is considered and when uncertainty due to load forecast error is also considered.

Incorporating Uncertainty Due to Unit Outage

Each generating unit is considered as a two-state model, according to which a unit is either available or unavailable for generation. According to this model, the unavailability of the generating unit i during a short time interval LT (known as the system lead time) is given by

$$U_i(LT) = 1 - e^{-\lambda_i LT} \quad (10)$$

where λ_i is the failure rate of unit i [14]. The probability $U_i(LT)$ given by (10) is known as the outage replacement rate (ORR) of the unit, i.e., probability of losing capacity and not being able to replace it.

To calculate the LOLP and EUE indices for every chromosome, the conventional "loss of load" method is used, except that ORR is used instead of forced outage rate (FOR).

This method is based on the creation of the capacity outage probability table (COPT) according to the given load curve [15]. A COPT is formed for every hour using the ORR of the committed units. The creation of COPT is based on the unit addition algorithm [15]. A COPT may be visualized as a table with n rows ($j = 1 \dots n$) and 3 columns. The first column represents n different generation levels that may be outaged. The second and third column represents the probability PR_j and total capacity CR_j that remains in service corresponding to each outage level, respectively. The reliability indices are calculated as follows: The LOLP index for each hour t is calculated as

$$LOLP_t = \sum_{j=1}^n (PR_j LOSS_j), \quad t \in [1, T] \quad (11)$$

where $LOSS_j$ is given by

$$LOSS_j = \begin{cases} 1, & \text{if } CR_j < LOAD_t \\ 0, & \text{otherwise.} \end{cases} \quad (12)$$

Similarly, the EUE index for each hour t is calculated as

$$EUE_t = \sum_{j=1}^n PR_j LOSS_j (LOAD_t - CR_j), \quad t \in [1, T]. \quad (13)$$

The EUE index of the dispatch period is given by EUE_{tot} which is calculated as

$$EUE_{tot} = \sum_{t=1}^T EUE_t. \quad (14)$$

Incorporating Uncertainty Due to Load Forecast Error

Load forecast may be associated with uncertainty and hence plays a major role in the solution of the TGS problem. It is an accepted practice to assume that the load forecast uncertainty can be reasonably described by a normal distribution [14], [15]. The distribution can be divided into a discrete number of class intervals with the distribution mean being the forecast load. The load representing the class interval mid-point is assigned the designated probability for that class interval. It is recommended in [15] that a seven-step approximation ($0, \pm 1\sigma, \pm 2\sigma, \pm 3\sigma$) to the normal distribution (seven-step model) is adequate to represent the uncertainty in load forecast. The standard deviation (σ or S) is a percentage of the expected demand (distribution mean) and is suggested to be 5% [16]. With the assumption of load forecast uncertainty to be normally distributed and represented by the seven-step model, the LOLP and EUE index calculation for each hour t is given by the following equations:

$$LOLP_t = \sum_{m=1}^7 (LOLP_t(m) PL(m)), \quad t \in [1, T] \quad (15)$$

$$EUE_t = \sum_{m=1}^7 (EUE_t(m) PL(m)), \quad t \in [1, T] \quad (16)$$

where $PL(m)$ indicates the probability associated with the discrete class interval m in the seven-step model. Similarly, $LOLP_t(m)$ and $EUE_t(m)$ represent the LOLP and EUE for each discrete class interval m for hour t .

Computational Time

The computational time in creating COPT is reduced by omitting the outage levels for which the cumulative probabilities are less than a predefined limit, e.g., 10^{-7} [14]. Additionally, to avoid the need for repeated creation of COPT, a memory archive is created to store the commitment patterns for each time period, and their corresponding LOLP and EUE index values. In subsequent generations, whenever a commitment pattern is repeated, the corresponding LOLP and EUE values are copied and assigned to the repeated pattern. This technique significantly reduces the computational time. It is noticed that calculation of the reliability indices of a chromosome is a bottleneck in terms of computation time. Hence, to further improve the computational speed, parallel computing is implemented and the hourly LOLP and EUE values of a chromosome are computed in parallel.

D. Repair Process

If a chromosome violates the load demand equality constraint, then a heuristic based repair operator is employed which was found to be efficient in our earlier study [1]. In case studies 2 and 3, in which emission cost is an objective, the chromosomes are repaired using priority list (PL) [17] based on either fuel cost coefficients or emission cost coefficients (with equal probability). In case study 1, in which emission cost is not considered as an objective, the chromosomes are repaired using PL based on just fuel cost coefficients.

E. Constraint Violation Evaluation

In this paper all the constraints have been normalized because different constraints make take different orders of magnitude. An inequality constraint of the form $g(x) \geq b$ is normalized using the following transformation:

$$\frac{g(x)}{b} - 1 \geq 0. \quad (17)$$

Equality constraints are also normalized similarly [19]. Since all normalized constraint violations take more or less the same order of magnitude, they are simply added to calculate the overall constraint violation of a chromosome. A chromosome is feasible if the overall constraint violation is less than 10^{-5} .

F. Objective Function Evaluation

The objective functions system operation cost (F_1) and emission cost (F_3) are calculated for each chromosome using its Res.PM while objective function F_2 is equal to the EUE index (EUE_{tot}).

G. Ranking and Selection

The chromosomes are ranked using the constrained-domination principle. Thereafter, constrained-binary tournament method is employed for selection [18].

H. Crossover

The TGS involves both discrete binary variables and continuous real variables. Hence, binary and real crossover operators are employed to explore both the search spaces. Standard crossover operators do not work well on the binary variables in the TGS problem [4]. Here, a slightly modified version of the window crossover operator as mentioned in [4] is used as the binary crossover. It works by randomly selecting two parents from the mating pool and then randomly selecting a window size. The entries within the window portion are exchanged between the UCM of two parents to generate the UCM of two offsprings. SBX crossover operator [19] is chosen as the real crossover operator and is applied on the RPM of two parents to obtain the RPM of two offsprings.

I. Mutation

1) *Swap-Window Operator*: The binary and real versions of this operator are applied separately on UCM and RPM of a chromosome respectively. It randomly selects: 1) two units u_1 and u_2 , 2) a time window of width w (hours) between 1 and T_{max} and 3) a window position. The entries of the two units u_1 and u_2 included in the window are then exchanged. This acts like a sophisticated mutation operator [2].

2) *Window Mutation Operator*: This operator works on the UCM of a chromosome by randomly selecting 1) a unit, 2) a time window of width w (hours) between 1 and T_{max} and 3) a window position. Then it mutates all the bits included in the window, turning all of them to either 1's or all of them to 0's with an equal probability [2].

The steps of MOGSA are described as follows:

- 1) **Parameter-setting input**: Population size, generation number, L_{max} , E_{max} , $Cost_{max}$, $Emission_{max}$, crossover probability, distribution index for SBX crossover, swap-window operator probability, window mutation operator probability.
- 2) **Initialization**: In the initial population, UCM and RPM of all chromosomes are randomly generated.
- 3) **Calculation of reliability indices**: The conventional "loss of load" method is used to calculate the LOLP and EUE indices of all chromosomes.
- 4) **Repair process**: Heuristic based repair operator is used to repair the chromosomes for load demand equality constraint violation.
- 5) **Constraint violation evaluation**: Normalized constraint violation (min up-down time, load demand, LOLP, EUE, Cost and Emission) is calculated and summed up for each chromosome.
- 6) **Objective function evaluation**: UCM and RPM of each chromosome are multiplied to form the resultant power matrix (Res.PM). The objective functions F_1 and F_3 are then calculated using the Res.PM and objective function F_2 is equal to the EUE index.
- 7) **Ranking and selection**: The population is ranked using the constrained-domination principle. Thereafter, constrained-binary tournament selection is used to form the mating pool.

TABLE I
PARAMETER SETTINGS

Population size	300
Generation number	10000
Crossover probability	0.6
Variable crossover probability in SBX	1
Distribution index in SBX	2
Swap window operator probability	0.25
Window mutation operator probability	0.25

- 8) **Crossover:** Crossover works by randomly selecting two parent chromosomes from the mating pool. Window crossover operator is applied on the UCM and SBX crossover operator on the RPM of the two parent chromosomes to form the UCM and RPM of the two offspring chromosomes.
- 9) **Mutation:** Swap-window operator and window-mutation operator are then applied on the offspring chromosomes.
- 10) **Calculation of reliability indices, repair process, constraint violation and objective function evaluation:** Steps 3–6 are performed for the offspring population.
- 11) **Ranking of combined population:** The parent population and offspring population are then combined and ranked according to the constrained-domination principle.
- 12) **Replacement:** The next generation is formed using the best chromosomes (with respect to fitness and spread) in the combined population.
- 13) **Termination:** If termination condition is satisfied then trade-off non-dominated solutions are obtained else steps 7) to 12) are repeated.

IV. CASE STUDIES AND DISCUSSIONS

In this paper, three case studies are performed using MOGSA on the TGS problem in uncertain environment considering different optimization models. The dispatch period considered in all the case studies is 24 hours. It is noted that L_{max} is given in percent (%) whereas EUE and E_{max} are expressed as a percentage of the expected energy demand of the total dispatch period. The lead time of the system is fixed as 4 hours for all case studies [14]. All simulations are performed using C platform on a PC with Intel Xeon 2.53-GHz processor and 12 GB of memory.

A. Case Study 1: Bi-Objective Optimization—System Operation Cost and Reliability (EUE) as Two Conflicting Objectives With LOLP as Constraint

In this case study, the TGS problem is solved in uncertain environment considering a bi-objective optimization model of minimizing system operation cost along with maximizing reliability (minimizing EUE). This optimization model can be useful for system operators who look for a reliable generation schedule while considering the economic objective. A test system of 26 thermal units is chosen for this case study [14].

The parameter settings of the algorithm obtained from experiments for this case study are as shown in Table I. The computational time requirement of MOGSA in this case study is around 40 min.

In the following sections, the effect of LOLP constraint and load forecast uncertainty is analyzed.

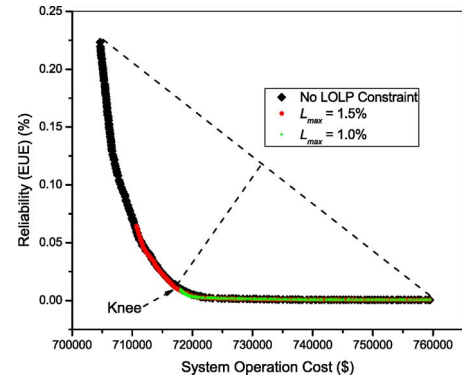


Fig. 1. P-O fronts for system operation cost v/s reliability (EUE) for 26 unit system considering unit unavailability for different L_{max} values.

1) *Effect of LOLP Constraint:* Simulations are performed at first considering the uncertainty due to unit outage alone. “Pareto-optimal” (P-O) fronts are obtained for no-LOLP constraint, $L_{max} = 1.5\%$ and 1.0% case as shown in Fig. 1. Fig. 1 shows that as the LOLP constraint gets stricter (i.e., L_{max} decreases), the solutions obtained are of lesser EUE objective value and higher cost.

It is interesting to note from the figure that a knee region exists for the given problem. This region is important in MOO problems as it consists of solutions with the maximum marginal rates of return, i.e., solutions for which a small improvement in one objective would lead to a large deterioration in the other objective [20]. Such characteristic of the knee solutions make them unique to decision makers for practical applications. A knee region can be visually identified as a convex bulge in the P-O front [20]. According to Das [21], knee on the P-O front corresponds to farthest solution from the line formed by joining the extreme solutions on the P-O front as shown in Fig. 1. The neighboring solutions to the knee on the P-O front are called the knee solutions.

It can be seen from Fig. 1 that a good representation of solutions is obtained on the cost-reliability (EUE) P-O front for no-LOLP constraint case. This P-O front offers the system operators to choose any optimum solution from the wider range of cost-reliability trade-off solutions. The corresponding LOLP values for the chosen solution can be determined for every hour. However, when the problem is constrained with $L_{max} = 1.5\%$ and 1.0% , the region of non-dominated solutions is limited as can be seen in Fig. 1. Fig. 1 depicts that the knee region lying above the knee is lost if an arbitrary value is assigned for L_{max} , as observed with $L_{max} = 1.0\%$.

However, as $L_{max} = 1.5\%$ constraint is found to cover the knee region, rest of the simulations in this paper consider $L_{max} = 1.5\%$. It is noted that L_{max} is a user-defined limit and can be set to any value as desired by the user.

2) *Effect of Load Forecast Uncertainty:* Simulations are further performed by incorporating uncertainty due to both unit outage and load forecast error in this study. Fig. 2 shows the P-O fronts corresponding to $L_{max} = 1.5\%$ constraint and standard deviation (S) of 1%, 3% and 5% in load forecast uncertainty. It can be observed that the P-O front obtained for lower S value dominates the P-O front obtained for higher S value. The

TABLE II
COMPARISON OF BEST COST AND SPINNING RESERVE FOR DIFFERENT EUE VALUES AND LOAD FORECAST UNCERTAINTIES

EUE (%)	S = 1%			S = 3%			C7 = (C4 - C1) Increase in Cost (\$)	S = 5%			C11 = (C8 - C4) Increase in Cost (\$)
	C1 Best Cost (\$)	C2 Spinning Reserve (MW)	C3 Spinning Reserve (%)	C4 Best Cost (\$)	C5 Spinning Reserve (MW)	C6 Spinning Reserve (%)		C8 Best Cost (\$)	C9 Spinning Reserve (MW)	C10 Spinning Reserve (%)	
0.03	714082	8172	14.88	714978	8494	15.47	896	717279	9255	16.85	2301
0.02	715734	8742	15.92	716920	9110	16.59	1186	720553	10156	18.50	3633
0.01	718001	9418	17.15	720826	10219	18.61	2825	727909	11790	21.47	7083

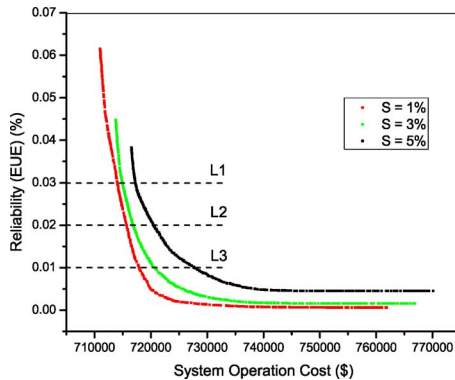


Fig. 2. P-O fronts for system operation cost v/s reliability (EUE) for 26 unit system considering unit unavailability and different values of load forecast uncertainty and $L_{max} = 1.5\%$.

reason behind the shift in P-O fronts as the load forecast uncertainty increases can be analyzed from Table II. For example, consider the horizontal line L1 in Fig. 2 that is drawn corresponding to $EUE = 0.03$. The solutions just below the line L1 on the three P-O fronts are compared for cost and system spinning reserve (SSR). It can be observed from Table II that for a particular EUE objective value (in this example 0.03), as the load forecast uncertainty increases; more SSR gets scheduled automatically to maintain the reliability level (close to $EUE = 0.03$ here) and thus results in higher cost. The solution's cost corresponding to $EUE = 0.03$ increases by \$896 with increase in load forecast uncertainty from $S = 1\%$ to $S = 3\%$ (as shown in column C7 of Table II) and increases by further \$2301 with increase in load forecast uncertainty from $S = 3\%$ to $S = 5\%$ (as shown in column C11 of Table II). Similar observations from rows corresponding to $EUE = 0.02$ and 0.01 show that the increase in solution's cost with increase in load forecast uncertainty is considerably higher if the desired reliability level is higher (i.e., EUE is lower). This illustrates the importance of accurate load forecasting as the amount of savings that can be made with better load forecasting is substantial.

To analyze solutions on a particular P-O front, the front corresponding to $S = 1\%$ is chosen here. Three horizontal lines L1, L2 and L3 are drawn corresponding to $EUE = 0.03$, 0.02 and 0.01 . The solutions on the P-O front just below these lines are compared for their cost and SSR. Table II shows that for a particular case of load forecast uncertainty (in this example $S = 1\%$), as the solution's reliability level increases (i.e., EUE value decreases); its scheduled SSR also increases which results in higher cost. The increase in solution's cost when EUE value decreases from 0.03 to 0.02 is \$1652 and the increase is

\$2267 with further decrease in EUE from 0.02 to 0.01 . This kind of comparison demonstrates to the SO that how much exactly he/she should compromise in cost to attain higher level of reliability.

In literature, generally most of the studies adopt deterministic criteria for evaluating the SSR requirements. For example, the most common criteria adopted in practice are that the reserve should be at least equal to the capacity of the largest unit or a specific percentage of the hourly system load. Such deterministic approaches have the disadvantage of not being able to consider the uncertainties in the problem. However, it is noted that the SSR gets scheduled automatically in the presented approach according to the desired level of reliability as discussed above.

3) *Comparison and Discussion:* In this section, the results obtained above are compared with the results presented in the study of Simopoulos *et al.* [14] where the TGS problem was solved considering system operation cost as the single objective with reliability (LOLP and EUE) as constraint. The authors in study [14] used SA for finding the optimum schedule of the generating units while the economic dispatch problem was solved separately for each hour through a quadratic programming routine.

The significance of setting reliability (EUE) as an objective (rather than a constraint) and the motivation behind solving the TGS as a MOO problem is explained in the following comparison and discussion. For comparison, the P-O front corresponding to $S = 5\%$, $L_{max} = 1.5\%$ is chosen here and shown in Fig. 3. The same problem was solved in study [14] with $E_{max} = 0.05\%$ constraint. It can be seen that all the solutions contained in the P-O front in Fig. 3 satisfy the constraint of $E_{max} = 0.05\%$. The region lying above the line L1 in the P-O front is expanded and shown in Fig. 4.

In Fig. 4, the vertical line L1 on the left coincides with the best cost solution (\$716 536) obtained from our proposed approach while the vertical line L2 on the right coincides with the best cost solution (\$716 862) obtained in the study [14]. It is noted that though both the best cost solution obtained in study [14] and in our proposed approach meet the constraint of $E_{max} = 0.05\%$, our result is better by \$326. Thus, if the SO decides to choose our best cost solution then the annual savings in comparison to the single-objective optimization methodology in [14] can be as much as $(\$326 \times 30 \times 12)$ i.e., \$117 360 which is quite significant. The generation schedule and corresponding costs for our best cost solution (\$716 536) are shown in Table III. Further, it is also observed from Fig. 4 that there are many solutions in between the two vertical lines obtained from our proposed

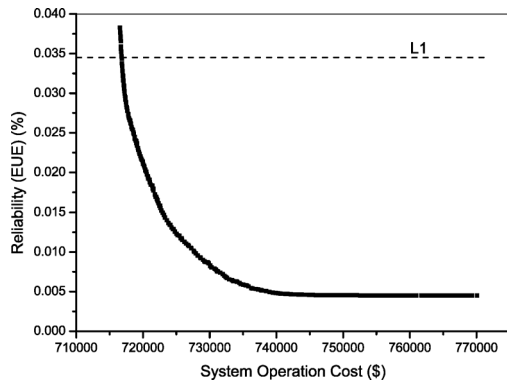


Fig. 3. P-O front for cost v/s reliability (EUE) for 26 unit system considering unit unavailability, $S = 5\%$ load forecast uncertainty and $L_{max} = 1.5\%$.

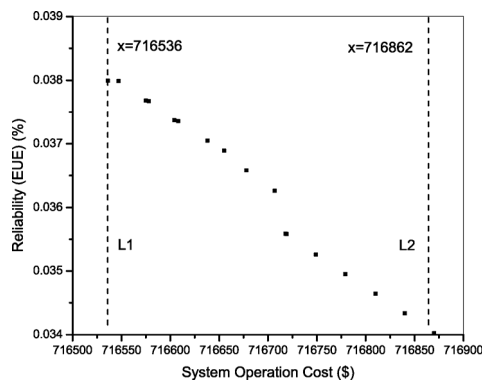


Fig. 4. Enlarged view of the region lying above line L1 in Fig. 3.

multi-objective approach which are better than the best cost solution obtained in the study [14].

Another important advantage of setting reliability (EUE) as an objective is that the complete trade-off P-O solutions between cost and reliability (EUE) are obtained in one single run of MOGSA. The P-O front exactly shows the nature of the trade-off between cost and reliability and by comparing solutions on a particular P-O front (as we demonstrated earlier), the SO can comprehend that exactly how much he/she should compromise in cost to achieve higher reliability.

Considering the uncertainty due to both unit outage and load forecast error, the best solution (in terms of cost) obtained using MOGSA is compared against the best solution obtained in study [14] by performing ten simulations for different cases as shown in Table IV. It can be observed from Table IV that MOGSA performed better than the benchmark in terms of best cost and average cost in all the cases. The worst cost for the ten runs was also better than the benchmark except in one case. This shows the robustness and the consistency of MOGSA in solving the TGS problem in uncertain environment.

B. Case Study 2: Bi-Objective Optimization—System Operation Cost and Emission Cost as Two Conflicting Objectives With Reliability (LOLP and EUE) as Constraint

In this case study, the TGS problem is solved in uncertain environment considering a bi-objective optimization model of

minimizing system operation cost and emission cost. The uncertainties relating to unit outage and load forecast error are incorporated by implementing reliability (LOLP and EUE) constraints. This optimization model can be useful for the system operator where the environmental aspect is equally important as the economic objective and the system operator is satisfied with the solution that meets the reliability constraint. A test system of 60 thermal units is chosen for this case study and the results are compared with our earlier study [1] in which the (same) bi-objective TGS problem was solved on the same test system in a deterministic environment.

The parameter settings for this case study are same as shown in Table I except that the generation number is 50 000. The computational time requirement of MOGSA in this case study is around 90 minutes. Fig. 5 shows the obtained P-O fronts for system operation cost and emission cost as objectives and with reliability constraint ($E_{max} = 0.05\%$, $L_{max} = 1.5\%$) for different load forecast uncertainties ($S = 1\%$, 3% and 5%). Fig. 5 also shows the comparison of results with the results obtained in our earlier work for the deterministic environment [1]. It is noted that in study [1], the SSR constraint was imposed to be minimum 10% of the load demand in each hour.

It can be observed from Fig. 5 that the P-O front obtained for lesser S value dominates the P-O front obtained for higher S value as was observed earlier in the case study 1 (in Fig. 2). The reason is now known from the case study 1 that as the load forecast uncertainty increases, more SSR gets scheduled. Fig. 5 also shows that the P-O fronts obtained for the uncertain environment dominate the P-O front obtained in our earlier study for the deterministic environment [1]. This provides an important indication that the deterministic criteria of implementing SSR (minimum 10% of the load demand in each hour) schedules more reserve than required even when considering the unavailability of generating units and load forecast uncertainty ($S = 1\%$, 3% , 5%). In a broader context, it also suggests that the deterministic criteria may be sometimes too conservative.

To quantitatively analyze the effect of load forecast uncertainty on the considered bi-objective optimization problem, two horizontal lines are drawn corresponding to emission cost of \$2 150 000 and \$2 100 000 and the solutions on different P-O fronts shown in Fig. 5 are compared for system operation cost. The comparative results are presented in Table V. It can be observed from Table V that for both the cases the increment in system operation cost with increase in load forecast uncertainty is considerably large. This again illustrates the importance of accurate load forecasting as the amount of savings that can be made with better load forecasting is substantial. Further, Table V also shows quantitatively how much the results obtained using our proposed multi-objective approach are better than the results obtained in our earlier study [1] in deterministic environment.

C. Case Study 3: Three-Objective Optimization—System Operation Cost, Emission Cost and Reliability (EUE) as Three Conflicting Objectives With LOLP as Constraint

In this case study, the TGS problem is solved in uncertain environment considering system operation cost, emission cost and reliability as objectives. This case study may be of significance to those system operators for whom the economic objective,

TABLE III
GENERATION SCHEDULE AND CORRESPONDING COSTS OF THE BEST COST SOLUTION FOR THE 26 UNIT SYSTEM

Units	Hours (1-24)																								Total
	1	2	3	4	5	6	7	8	9	10	11	12	13	14	15	16	17	18	19	20	21	22	23	24	
1	0.0	0.0	0.0	0.0	0.0	0.0	2.4	2.4	0.0	2.4	2.4	0.0	0.0	0.0	0.0	2.4	0.0	0.0	0.0	0.0	0.0	0.0	0.0	0.0	
2	0.0	0.0	0.0	0.0	0.0	0.0	2.4	0.0	0.0	0.0	2.4	0.0	0.0	0.0	2.4	2.4	0.0	0.0	0.0	0.0	0.0	0.0	0.0	0.0	
3	0.0	0.0	0.0	0.0	0.0	0.0	2.4	0.0	0.0	0.0	2.4	0.0	0.0	0.0	0.0	2.4	0.0	0.0	0.0	0.0	0.0	0.0	0.0	0.0	
4	0.0	0.0	0.0	0.0	0.0	0.0	0.0	0.0	0.0	0.0	2.4	0.0	0.0	0.0	0.0	0.0	0.0	0.0	0.0	0.0	0.0	0.0	0.0	0.0	
5	0.0	0.0	0.0	0.0	0.0	0.0	0.0	0.0	0.0	0.0	2.4	0.0	0.0	0.0	0.0	0.0	0.0	0.0	0.0	0.0	0.0	0.0	0.0	0.0	
6	0.0	0.0	0.0	0.0	0.0	0.0	0.0	0.0	0.0	0.0	0.0	0.0	0.0	0.0	0.0	0.0	0.0	0.0	0.0	0.0	0.0	0.0	0.0	0.0	
7	0.0	0.0	0.0	0.0	0.0	0.0	0.0	0.0	0.0	0.0	0.0	0.0	0.0	0.0	0.0	0.0	0.0	0.0	0.0	0.0	0.0	0.0	0.0	0.0	
8	0.0	0.0	0.0	0.0	0.0	0.0	0.0	0.0	0.0	0.0	0.0	0.0	0.0	0.0	0.0	0.0	0.0	0.0	0.0	0.0	0.0	0.0	0.0	0.0	
9	0.0	0.0	0.0	0.0	0.0	0.0	0.0	0.0	0.0	0.0	0.0	0.0	0.0	0.0	0.0	0.0	0.0	0.0	0.0	0.0	0.0	0.0	0.0	0.0	
10	15.2	15.2	15.2	15.2	15.2	15.2	60.2	76.0	76.0	76.0	76.0	76.0	76.0	76.0	76.0	76.0	76.0	76.0	76.0	76.0	76.0	76.0	76.0	15.2	
11	15.2	15.2	15.2	15.2	15.2	15.2	39.0	76.0	76.0	76.0	76.0	76.0	76.0	76.0	76.0	76.0	76.0	76.0	76.0	76.0	76.0	76.0	76.0	15.2	
12	15.2	15.2	15.2	15.2	15.2	15.2	46.4	76.0	76.0	76.0	76.0	76.0	76.0	76.0	76.0	76.0	76.0	76.0	76.0	76.0	76.0	76.0	76.0	15.2	
13	0.0	0.0	0.0	0.0	15.2	15.2	27.1	76.0	76.0	76.0	76.0	76.0	76.0	76.0	76.0	76.0	76.0	76.0	76.0	76.0	76.0	76.0	58.1	15.2	
14	0.0	0.0	0.0	0.0	0.0	25.0	25.0	73.5	100.0	100.0	100.0	100.0	100.0	100.0	100.0	100.0	100.0	100.0	100.0	100.0	100.0	100.0	25.0	25.0	
15	0.0	0.0	0.0	0.0	0.0	0.0	25.0	90.7	80.8	100.0	100.0	100.0	100.0	85.7	100.0	100.0	96.3	73.3	90.5	97.7	100.0	71.0	25.0	0.0	
16	0.0	0.0	0.0	0.0	0.0	0.0	0.0	51.5	78.4	100.0	100.0	100.0	100.0	83.4	100.0	100.0	72.9	75.8	28.7	71.5	100.0	28.1	25.0	0.0	
17	155.0	155.0	140.9	140.6	155.0	155.0	155.0	155.0	155.0	155.0	155.0	155.0	155.0	155.0	155.0	155.0	155.0	155.0	155.0	155.0	155.0	155.0	155.0	155.0	
18	123.9	144.7	135.7	128.1	154.9	155.0	155.0	155.0	155.0	155.0	155.0	155.0	155.0	155.0	155.0	155.0	155.0	155.0	155.0	155.0	155.0	155.0	155.0	155.0	
19	106.2	115.8	104.8	119.5	119.7	155.0	155.0	155.0	155.0	155.0	155.0	155.0	155.0	155.0	155.0	155.0	155.0	155.0	155.0	155.0	155.0	155.0	155.0	155.0	
20	119.3	118.9	113.0	116.2	109.6	149.2	155.0	155.0	155.0	155.0	155.0	155.0	155.0	155.0	155.0	155.0	155.0	155.0	155.0	155.0	155.0	155.0	155.0	139.2	
21	0.0	0.0	0.0	0.0	0.0	0.0	69.0	69.0	69.0	85.7	105.1	78.1	78.1	69.0	105.7	130.9	69.0	69.0	69.0	69.0	69.0	69.0	69.0	0.0	
22	0.0	0.0	0.0	0.0	0.0	0.0	69.0	69.0	69.0	109.9	69.0	69.0	69.0	69.0	69.0	69.0	69.0	69.0	69.0	69.0	69.0	69.0	69.0	0.0	
23	0.0	0.0	0.0	0.0	0.0	0.0	0.0	0.0	69.0	69.0	69.0	69.0	69.0	69.0	69.0	69.0	69.0	69.0	69.0	69.0	69.0	69.0	69.0	0.0	
24	350.0	350.0	350.0	350.0	350.0	350.0	350.0	350.0	350.0	350.0	350.0	350.0	350.0	350.0	350.0	350.0	350.0	350.0	350.0	350.0	350.0	350.0	350.0	350.0	
25	400.0	400.0	400.0	400.0	400.0	400.0	400.0	400.0	400.0	400.0	400.0	400.0	400.0	400.0	400.0	400.0	400.0	400.0	400.0	400.0	400.0	400.0	400.0	400.0	
26	400.0	400.0	400.0	400.0	400.0	400.0	400.0	400.0	400.0	400.0	400.0	400.0	400.0	400.0	400.0	400.0	400.0	400.0	400.0	400.0	400.0	400.0	400.0	400.0	
Power (MW)	1700.0	1730.0	1690.0	1700.0	1750.0	1850.0	2000.0	2430.0	2540.0	2600.0	2670.0	2590.0	2590.0	2550.0	2620.0	2650.0	2550.0	2530.0	2500.0	2550.0	2600.0	2480.0	2200.0	1840.0	54910.0
Fuel Cost (\$)	18556	18914	18436	18553	19262	20836	23400	32151	34763	36027	37797	35763	35763	34955	36497	37265	34956	34573	34013	34956	35997	33631	27305	20714	715084.3
Start-up Cost (\$)	0	0	0	0	81.2	130.5	130.5	783.4	326.4	0	0	0	0	0	0	0	0	0	0	0	0	0	0	0	1452.1

TABLE IV
COMPARISON FOR VARIOUS RELIABILITY LEVELS AND LOAD FORECAST UNCERTAINTY VALUES

E_{max} (%)	L_{max} (%)	S (%)	Best Cost (\$)	Best Cost (benchmark) (\$) [14]	Diff. (\$)	Av. Cost (\$)	Avg. Cost (benchmark) (\$) [14]	Diff. (\$)	Worst Cost (\$)	Worst Cost (benchmark) (\$) [14]	Diff. (\$)
0.05	1.5	0	710678	712067	-1389	710700	712704	-2004	710760	713473	-2713
0.05	1.5	1	710948	712216	-1268	711349	712384	-1035	712912	712638	+274
0.05	1.5	3	712582	713855	-1273	713628	714119	-491	714102	714390	-288
0.05	1.5	5	716536	716862	-326	716651	717098	-447	716775	717318	-543

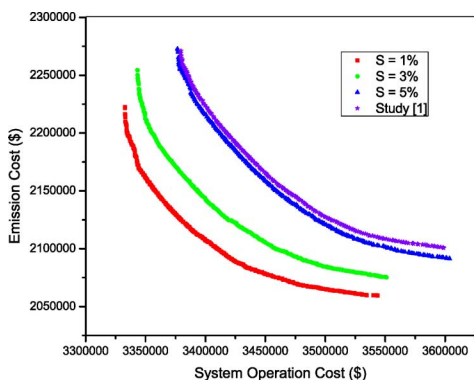


Fig. 5. P-O fronts for system operation cost v/s emission cost considering unit outage and different values of load forecast uncertainty for $E_{max} = 0.05\%$, $L_{max} = 1.5\%$ and comparison with our earlier study [1] on 60 unit system.

emission objective and reliability objective all are equally important and who would like to solve the TGS problem as a truly MOO problem to avail of trade-off opportunities thus offered.

TABLE V
COMPARISON OF SYSTEM OPERATION COST FOR DIFFERENT EMISSION COST AND LOAD FORECAST UNCERTAINTIES

	System operation cost and increment corresponding to emission cost of \$2150000		System operation cost and increment corresponding to emission cost of \$2100000	
	Cost (\$)	Increment (\$)	Cost (\$)	Increment (\$)
S = 1%	3358951	-	3414408	-
S = 3%	3394293	29553	3457087	42679
S = 5%	3460228	66257	3559383	102296
Study [1]	3467784	7506	3598844	39461

Simulation is performed considering the uncertainty due to both unit outage and load forecast error on the same test system of 60 units as used in case study 2. It is noted that since in this case study the objective space is relatively quite large (because of three objectives), the algorithm requires large population size as well. However, the authors' observed that the algorithm explores many solutions with very high reliability but with very high system operation cost and high emission cost which may not be that attractive to the system operator. Hence, the authors' introduce two additional constraints in this case study related

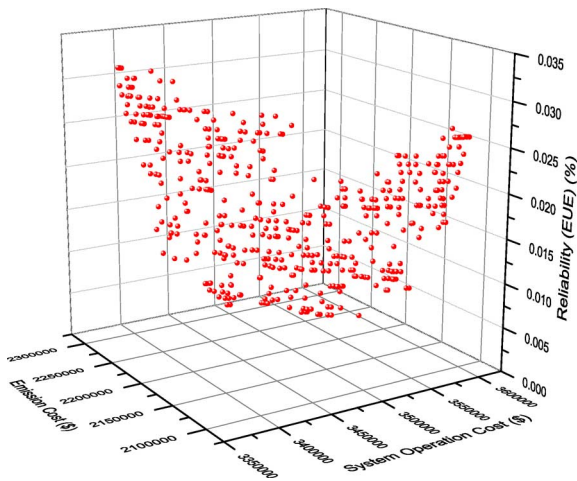


Fig. 6. P-O solutions for system operation cost v/s emission cost v/s reliability (EUE) for $L_{max} = 1.5\%$, $S = 5\%$, $Cost_{max} = \$3\,600\,000$ and $Emission_{max} = \$2\,300\,000$ on 60 unit system.

TABLE VI
RESULTS FOR HYPERVOLUME INDICATOR (I_H^-)

Case Study	Best	Median	Worst	Mean	Std.Dev.
1	0.0020	0.0026	0.0032	0.0026	0.0003
2	0.0065	0.0351	0.0821	0.0352	0.0216
3	0.0485	0.0565	0.0680	0.0568	0.0051

to maximum system operation cost (8) and maximum emission cost (9) so that the algorithm's resources (i.e., population) and time are not wasted in searching the undesirable solutions.

The parameter settings for this case study are same as shown in Table I except that the population size is 500 and generation number is 50 000. The values set for $Cost_{max}$ and $Emission_{max}$ are \$3 600 000 and \$2 300 000, respectively. The computational time requirement of MOGSA in this case study is around 3.75 hours. Fig. 6 shows the P-O solutions obtained for simultaneously optimizing the three objectives with $L_{max} = 1.5\%$ constraint and $S = 5\%$ load forecast uncertainty.

Now, the results obtained in this case study are compared with the results obtained in case study 2. The difference in these two case studies is that in this case study reliability (EUE) is an objective along with system operation cost and emission cost whereas it is a constraint ($E_{max} = 0.05\%$) in case study 2. Hence, in case study 2 the algorithm was directed towards finding non-dominated solutions that exhibited trade-off with respect to economic and emission objectives and satisfied the reliability constraint while in case study 3 the algorithm was directed towards finding non-dominated solutions that exhibited trade-off with respect to all the three objectives. It can be seen in Fig. 6 that all the P-O solutions satisfy the constraint of $E_{max} = 0.05\%$ as the P-O solutions in case study 2 did. However, the P-O solutions obtained in case study 2 cannot be distinguished on the basis of reliability as all solutions satisfy the same reliability constraints of $E_{max} = 0.05\%$ and $L_{max} = 1.5\%$ whereas the P-O solutions obtained in this case study exhibit a trade-off with respect to reliability too and cover a wide range of EUE (0.002–0.032) as can be seen in Fig. 6.

Hence, we can say that the P-O solutions obtained using the three-objective optimization model are more informative and provide more trade-off opportunities than the solutions obtained in case study 2.

SO may according to his/her preference choose to solve the TGS problem by considering any of the optimization model presented in this paper. However, based on the case studies presented in this paper, a systematic procedure is presented to choose a single solution for the TGS problem. It was observed in case study 1 that solutions with better cost are obtained by considering reliability as an objective rather than a constraint. Further, it was observed from the comparison of results obtained in case study 2 and 3 that solving the TGS as a reliability-constrained problem cannot present trade-off with respect to reliability. Hence, the authors' suggest that the TGS problem should be first solved as a truly MOO problem as in case study 3. After the non-dominated solutions are obtained as in Fig. 6, the SO may then according to his/her experience or choice put a constraint on reliability and eliminate the solutions not meeting the reliability constraint. This will leave the SO with a sub-set of solutions. The SO may then next put a constraint on emission cost and similarly eliminate the solutions not meeting the emission constraint. This will leave the SO with even smaller sub-set of solutions. The SO can then next just choose the solution with minimum system operation cost.

V. QUANTITATIVE PERFORMANCE ASSESSMENT

Multi-objective evolutionary algorithms are randomized search algorithms and stochastic in nature. Thus, if an MOEA is applied several times to the same problem, each time a different Pareto set may be returned. Therefore, there is a need to conduct performance assessment of the algorithm. In this paper, quantitative performance assessment of the proposed algorithm MOGSA has been done using hypervolume indicator (I_H^-) [22]. Hypervolume indicator (I_H^-) is a performance metric that measures the hypervolume of that portion of the objective space which is weakly dominated by the Pareto set found by the algorithm. This indicator evaluates the closeness and diversity achieved by the algorithm in a combined sense [19]. Hypervolume indicator (I_H^-) calculates the hypervolume difference of the Pareto set with respect to the reference set and smaller values of (I_H^-) (i.e., close to zero) correspond to higher quality [22]. MOGSA is executed for 25 runs with different initial population. The reference set is created by choosing the non-dominated solutions from union of non-dominated solutions over 25 runs. Hypervolume indicator (I_H^-) is evaluated for each of the three case studies and the quantitative performance assessment results are shown in Table VI. It is observed from Table VI that the best, worst, mean, median and standard deviation of (I_H^-) lies close to zero in each of the three case studies. This shows consistent performance of MOGSA over 25 different runs in each of the three case studies and validates the stability of the proposed algorithm.

VI. CONCLUSION

System operators generally solve the day-ahead TGS problem as a constrained single-objective optimization problem in deterministic environment. In this paper, we presented a

realistic multi-objective approach for solving the day-ahead TGS problem in uncertain environment. We proposed three different MOO models that may be chosen by the SO according to his/her own preference.

Overall, solving the TGS as a realistic MOO problem in uncertain environment using the presented approach provides the following advantages to the SO. In one single run of MOGSA, the entire P-O front is obtained that not only provides solution with better cost (as compared to solving the problem as a constrained single-objective optimization problem) but also presents a trade-off with emission cost or/and reliability (depending upon the optimization model). Moreover, the SSR gets scheduled automatically according to the level of reliability.

This paper discussed various advantages in solving the TGS problem as a realistic MOO problem in uncertain environment that should convince the SO to adopt the proposed multi-objective approach. The paper also demonstrated efficacy and consistent performance of MOGSA in solving the day-ahead TGS problem in uncertain environment for diverse set of objectives.

REFERENCES

- [1] A. Trivedi, N. M. Pindoriya, D. Srinivasan, and D. Sharma, "Improved multi-objective evolutionary algorithm for day-ahead thermal generation scheduling," in *Proc. Congr. Evol. Comput.-CEC'11*, New Orleans, LA, 2011, pp. 2170–2177.
- [2] S. A. Kazarlis, A. G. Bakirtzis, and V. Petridis, "A genetic algorithm solution to the unit commitment problem," *IEEE Trans. Power Syst.*, vol. 11, pp. 83–92, 1996.
- [3] I. G. Damousis, A. G. Bakirtzis, and P. S. Dokopoulos, "A solution to the unit-commitment problem using integer-coded genetic algorithm," *IEEE Trans. Power Syst.*, vol. 19, pp. 1165–1172, 2004.
- [4] J. Valenzuela and A. E. Smith, "A seeded memetic algorithm for large unit commitment problems," *J. Heuristics*, vol. 8, pp. 173–195, 2002.
- [5] T. O. Ting, M. V. C. Rao, and C. K. Loo, "A novel approach for unit commitment problem via an effective hybrid particle swarm optimization," *IEEE Trans. Power Syst.*, vol. 21, pp. 411–418, 2006.
- [6] A. H. Mantawy, Y. L. Abdel-Magid, and S. Z. Selim, "A simulated annealing algorithm for unit commitment," *IEEE Trans. Power Syst.*, vol. 13, pp. 197–204, 1998.
- [7] N. Sinha, R. Chakrabarti, and P. K. Chattopadhyay, "Evolutionary programming techniques for economic load dispatch," *IEEE Trans. Evol. Computat.*, vol. 7, pp. 83–94, 2003.
- [8] J.-B. Park, K.-S. Lee, J.-R. Shin, and K. Y. Lee, "A particle swarm optimization for economic dispatch with nonsmooth cost functions," *IEEE Trans. Power Syst.*, vol. 20, pp. 34–42, 2005.
- [9] M. A. Abido, "Multiobjective evolutionary algorithms for electric power dispatch problem," *IEEE Trans. Evol. Computat.*, vol. 10, pp. 315–329, 2006.
- [10] L. Wang and C. Singh, "Environmental/economic power dispatch using a fuzzified multi-objective particle swarm optimization algorithm," *Elect. Power Syst. Res.*, vol. 77, pp. 1654–1664, 2007.
- [11] S. Agrawal, B. K. Panigrahi, and M. K. Tiwari, "Multiobjective particle swarm algorithm with fuzzy clustering for electrical power dispatch," *IEEE Trans. Evol. Computat.*, vol. 12, pp. 529–541, 2008.
- [12] L. Wang and C. Singh, "Stochastic economic emission load dispatch through a modified particle swarm optimization algorithm," *Elect. Power Syst. Res.*, vol. 78, pp. 1466–1476, 2008.
- [13] L. Wang and C. Singh, "Unit commitment considering generator outages through a mixed-integer particle swarm optimization algorithm," *Appl. Soft Comput. J.*, vol. 9, pp. 947–953, 2009.
- [14] D. N. Simopoulos, S. D. Kavatzas, and C. D. Vournas, "Reliability constrained unit commitment using simulated annealing," *IEEE Trans. Power Syst.*, vol. 21, pp. 1699–1706, 2006.
- [15] R. Billinton and R. N. Allan, *Reliability Evaluation of Power Systems*. London, U.K.: Plenum, 1996.
- [16] R. N. Allan, R. Billinton, and N. M. K. Abdel-Gawad, "The IEEE reliability test system—Extensions to and evaluation of the generating system," *IEEE Trans. Power Syst.*, vol. 1, pp. 1–7, 1986.
- [17] T. Senjyu, K. Shimabukuro, K. Uezato, and T. Funabashi, "A fast technique for unit commitment problem by extended priority list," *IEEE Trans. Power Syst.*, vol. 18, pp. 882–888, 2003.
- [18] K. Deb, A. Pratap, S. Agarwal, and T. Meyarivan, "A fast and elitist multiobjective genetic algorithm: NSGA-II," *IEEE Trans. Evol. Computat.*, vol. 6, pp. 182–197, 2002.
- [19] K. Deb, *Multi-Objective Optimization Using Evolutionary Algorithms*. Singapore: Wiley, 2001.
- [20] L. Rachmawati and D. Srinivasan, "Multiobjective evolutionary algorithm with controllable focus on the knees of the Pareto front," *IEEE Trans. Evol. Computat.*, vol. 13, pp. 810–824, 2009.
- [21] I. Das, "On characterizing the 'knee' of the Pareto curve based on normal-boundary intersection," *Struct. Optimiz.*, vol. 18, pp. 107–115, 1999.
- [22] J. D. Knowles, L. Thiele, and E. Zitzler, A Tutorial on the Performance Assessment of Stochastic Multiobjective Optimizers, ETH Zurich, Tech. Rep., Feb. 2006.

Anupam Trivedi (S'10) received the dual degree (integrated Bachelor's and Master's) in civil engineering from the Indian Institute of Technology (IIT) Bombay, India, in 2009. Currently he is pursuing the Ph.D. degree in the Department of Electrical and Computer Engineering, National University of Singapore.

His research interest is in evolutionary algorithms, multi-objective optimization, and power system scheduling.

Dipti Srinivasan (M'89–SM'02) received the Ph.D. degree in engineering from the National University of Singapore in 1994.

She worked as a Postdoctoral Researcher at the University of California, Berkeley, from 1994 to 1995 before joining the National University of Singapore, where she is currently an Associate Professor in the Department of Electrical and Computer Engineering. Her research interest is the application of soft computing techniques to engineering optimization and control problems.

Deepak Sharma (S'07–M'09) received the Master's and Ph.D. degrees in mechanical engineering from the Indian Institute of Technology (IIT) Kanpur, India, in 2004 and 2010, respectively.

During his Doctoral studies at Université de Strasbourg, France, during 2009–2010 and National University of Singapore during 2010–2012, he specialized in optimization, specifically in evolutionary algorithms. Currently, he is an Assistant Professor in the Mechanical Engineering Department at IIT Guwahati, India. His main research interests include evolutionary algorithms, multi-objective optimization, and multidisciplinary design optimization.

Chanan Singh (S'71–M'72–SM'79–F'91) is currently Regents Professor and J. W. Runyon Chair Professor in the Department of Electrical and Computer Engineering at Texas A&M University (TAMU), College Station. His research and consulting interests are in the application of probabilistic methods to power systems.